Aftereffects of Nuclear Decay in $^{57}CoCl_2 \cdot nH_2O$ (n=2 and 6) Investigated by γ-X Ray Coincidence Mössbauer Spectroscopy

Takayuki KOBAYASHI*,† and Jean M. FRIEDT
Centre de Recherches Nucléaires, 67037 Strasbourg Cedex, France
(Received September 11, 1985)

The anomalous states produced by electron capture decay of ^{57}Co in $CoCl_2 \cdot 2H_2O$ and $CoCl_2 \cdot 6H_2O$ are investigated using conventional Mössbauer emission spectroscopy and a γ-X ray coincidence method which allows to isolate events with a reduced influence of the Auger electron self-irradiation. The formation of the anomalous electronic and structural configuration is assigned to the self-radiolysis of the water ligands. The mechanism involves both the nearest and the next nearest H_2O coordination shell according to the densities of these ligand molecules in the respective shells.

In insulating materials, doped or labelled with radioactive nuclei, anomalous valence or structural configurations of the decaying atoms are sometimes formed besides the normal state. This is called the aftereffect of nuclear decay which can be investigated very uniquely (in situ analysis on a time scale of the order of 100 ns after the decay) using Mössbauer emission spectroscopy.[1-6] One often invoked mechanism for these aftereffects considers that the chemical bonds in the immediate vicinity of the decaying atom are ruptured by the emitted photons and particles, e.g. the X-rays and Auger electrons emitted after the electron capture (EC) decay of ^{57}Co.[7] The resulting radicals hence formed around the atoms would play a determinant role in stabilizing the anomalous states. In the case of inorganic divalent compounds surrounded by water ligands it is considered that the formation of the anomalous trivalent Fe^{3+} arises mainly from free OH radicals produced by internal radiolysis of the H_2O ligands. This mechanism is simulated by γ-irradiation experiments of the Fe salt hydrates which for instance in the case of $FeSO_4 \cdot nH_2O$ (n=0,1,4,7) conclusively demonstrated the oxidation of Fe^{2+} by OH radicals:[8]

$$Fe^{2+} + OH \rightleftharpoons Fe^{3+} + OH^-. \quad (1)$$

However, the mechanisms of the aftereffects of nuclear decay are certainly more complicated than those of an external irradiation because of the superposition of primary excitations (direct ionization and excitation) and because of distribution in the particle flux and energy etc. In order to improve the understanding of those phenomena, it is desirable to modulate the conditions of the internal irradiation, i.e., to change the energy, intensity or the time involved in the processes. One possible approach relies on a γ-X ray coincidence technique, which allows to measure Mössbauer emission spectra corresponding to a reduced flux of Auger electrons after the EC decay of ^{57}Co. In this work we report a study, by using the γ-X ray coincidence technique, of the aftereffects in the hydrated compounds with water ligands; $CoCl_2 \cdot 2H_2O$ and $CoCl_2 \cdot 6H_2O$ labelled with ^{57}Co.

Experimental

Principle of the Experiment. After the EC decay of ^{57}Co, a K-X ray or K-Auger electron is emitted with the probability of approximately 30 or 60%, respectively.[9] The K-X ray emission causes one vacancy in the L or M shell, while two vacancies are produced in the L and/or M shells owing to the K-Auger effect. Each vacancy brings about the Auger cascade in the outer shells. Therefore, more (factor of $\approx$2) low-energy electrons are emitted during the Auger cascade after the K-Auger process than after the K-X ray emission. If a Mössbauer spectrum is observed, by the coincidence technique, i.e. only when K-X rays are emitted, the flux of the low-energy Auger electrons is reduced compared with that in the conventional Mössbauer emission method. By comparing the coincidence spectrum with the conventional one, it is expected to obtain new insights into the mechanisms of the aftereffects. This is the idea of the γ-X ray coincidence Mössbauer method, which is described elsewhere in more detail.[10,11]

Preparation of Samples. In order to avoid decomposition of the sample material during the measurements, very thin and little chemical compound ($CoCl_2 \cdot 2H_2O$ or $CoCl_2 \cdot 6H_2O$) labelled with ^{57}Co was surrounded with a large quantity of the same and unlabelled compound, and sealed between thin Mylar films. The intensity and specific activity of the sample source were approximately 10 μCi and 40 Ci mole^{-1}, respectively.

Measurements. The slow coincidence technique was used for the measurements, and the coincidence and conventional Mössbauer spectra were observed simultaneously at room temperature. The block diagram of the measuring system is shown in Fig. 1. The detectors used for 6.5 keV X-rays and 14.4 keV γ-rays were NaI(Tl) crystals with 1-inch diameter and 0.2-mm thickness. Since the resolving time of X-ray signals was approximately 4 μs, the universal coincidence unit was opened, for γ-rays, for sufficiently long time compared with the lifetime of the Mössbauer level and therefore the line-broadening due to the time effects[12,13] was considered to be negligible. In order to get a large geometrical efficiency, the sample source was placed just in front of the X-ray detector. The contribution of random coincidences was subtracted from the observed coincidence spectrum. The random coincidence counting rate was less than 20% of the total coincidence counting rate.

†Present address: Shiga University of Medical Science, Otsu, Shiga 520-21.

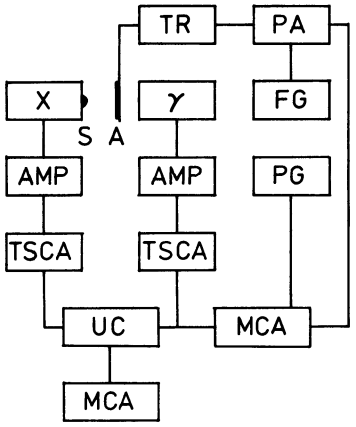

Fig. 1. Block diagram of the measuring system. S: sample source, A: absorber $Na_4Fe(CN)_6 \cdot 10H_2O$, X and γ:X- and γ-ray detectors, AMP: amplifier, TSCA: timing single channel analyzer, UC: universal coincidence, MCA: multichannel analyzer, TR: transducer, PA: power amplifier, FG: function generator, PG: pulse generator.

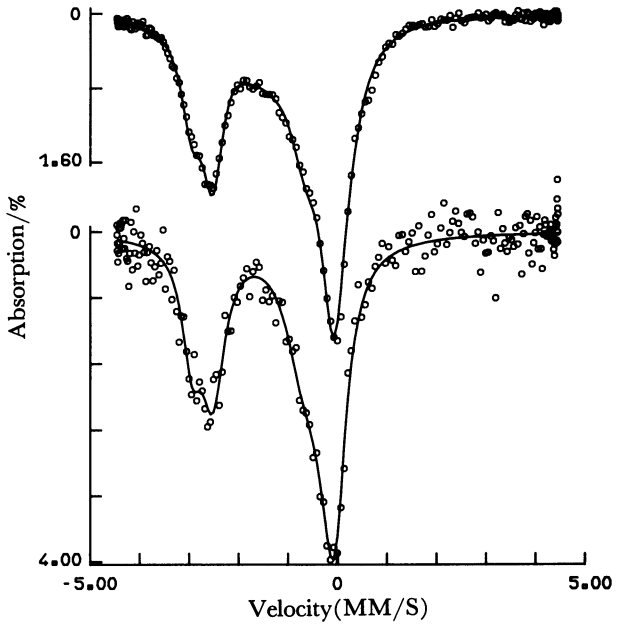

Fig. 2. Observed spectra of $CoCl_2 \cdot 2H_2O$. Upper and lower figures are the conventional and coincidence spectra with base-line counts of approximately 7.1×10^6 and 2.6×10^5, respectively.

Results

The observed spectra shown in Figs. 2 and 3 are composed of a large main peak and a small side peak, and were analyzed as a superposition of several Lorentzian lines. Rather good fits are obtained by assuming three symmetrical quadrupole doublets when the spectra are analyzed individually. However, in order to reach a consistent analysis of both the conventional and the coincidence data it appeared

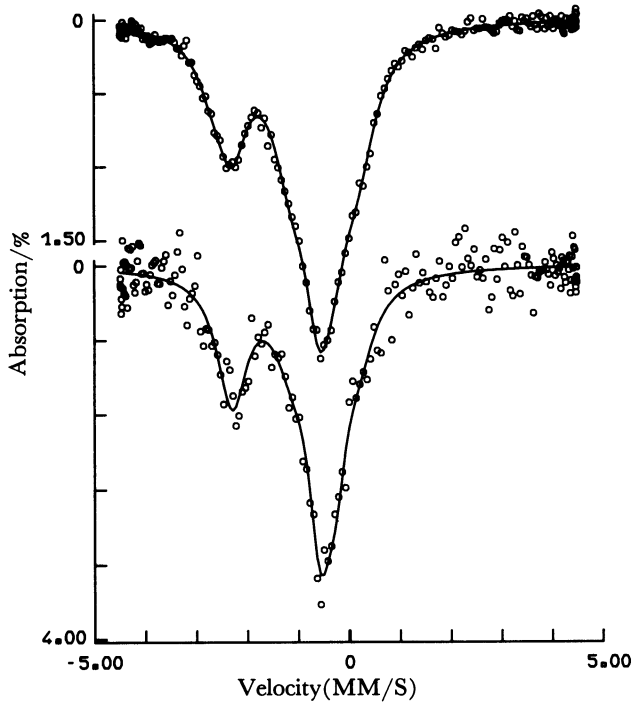

Fig. 3. Observed spectra of $CoCl_2 \cdot 6H_2O$. Upper and lower figures are the conventional and coincidence spectra with base-line counts of approximately 6.6×10^6 and 2.1×10^5, respectively.

necessary to introduce a number of conditions:

1) The hyperfine parameters of the several sites are equal in the coincidence and in the conventional spectra.

2) All the components in the coincidence spectrum must be found in the conventional spectrum, since the resonance absorption after X-ray emission contributes to the conventional spectrum as well as to the coincidence spectrum.

3) The line-width in the coincidence spectrum is equivalent to or less than the corresponding width in the conventional spectrum, because the defects of surroundings of ^{57}Fe after the decay of ^{57}Co under the coincidence conditions are expected to be reduced in comparison with the conventional measurements.

The good and simultaneous fits of the conventional and coincidence spectra are realized with the parameters in Table 1 which satisfy the above conditions.

In reference to the isomer shift (I.S.) and quadrupole splitting (Q.S.) of $FeCl_2 \cdot 2H_2O$[14] and $CoCl_2 \cdot 6H_2O$ doped with a small amount of Fe, the components Fe^{2+} (1) in Table 1 are attributed to the normal states in the lattice.

Discussion

The relative intensities of the components in the spectra are shown graphically in Fig. 4. The Fe^{2+}(1) contribution is greater in the coincidence spectrum than in the conventional one, reflecting the reduced influence of the low-energy electrons in the coincidence

Table 1. Mössbauer Parameters of the Conventional and Coincidence Spectra

State	I.S.	Q.S.	Conventional		Coincidence	
			width	intensity	width	intensity
	mm s^{-1}	mm s^{-1}	mm s^{-1}	%	mm s^{-1}	%
			$CoCl_2 \cdot 2H_2O$			
$Fe^{2+}(1)$	−1.31±0.02	2.42±0.03	0.53±0.01	35.1	0.59±0.05	43.4
$Fe^{2+}(2)$	−1.48±0.11	2.93±0.22	0.53±0.01	21.4	0.47±0.07	23.4
$Fe^{2+}(3)$	−1.54±0.04	0.45±0.05	0.81±0.03	8.3	—	—
$Fe^{3+}(1)$	−0.52±0.03	0.41±0.09	0.79±0.11	13.1	0.79±0.11	33.1
$Fe^{3+}(2)$	−0.23±0.01	0.80±0.02	0.81±0.03	22.2	—	—
			$CoCl_2 \cdot 6H_2O$			
$Fe^{2+}(1)$	−1.43±0.03	1.75±0.02	0.73±0.04	31.1	0.72±0.07	47.9
$Fe^{2+}(2)$	−1.71±0.05	1.93±0.08	0.73±0.04	10.0	—	—
$Fe^{3+}(1)$	−0.42±0.13	0.32±0.13	0.68±0.08	23.6	0.52±0.08	27.1
$Fe^{3+}(2)$	−0.48±0.08	1.30±0.10	0.88±0.03	35.2	0.83±0.09	24.9

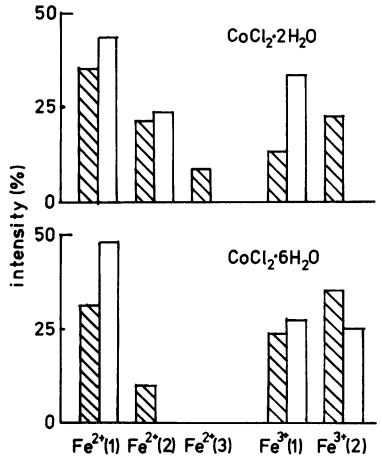

Fig. 4. Relative intensities of the components in the spectra. The slash marked and blank bars denote the results from the conventional and the coincidence spectra, respectively.

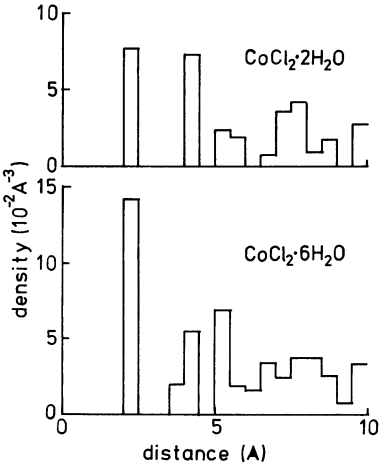

Fig. 5. Densities of H_2O molecules as a function of distance from a Co atom in $CoCl_2 \cdot 2H_2O$ and $CoCl_2 \cdot 6H_2O$.

spectrum. A mechanism for the appearance of the states other than $Fe^{2+}(1)$ is searched from consideration of the densities of H_2O molecules as a function of distance from a Co atom in the source materials (Fig. 5).

Many nearest neighbouring H_2O molecules exist in the hexahydrate. However, in the dihydrate the density of the second nearest neighbouring H_2O is equivalent to that of the nearest H_2O. Therefore, it is expected that the role of the second nearest H_2O in the aftereffects is relatively more important in the dihydrate than in the hexahydrate. The variety of the states in the dihydrate (Fig. 4) is assigned to the effect of these further H_2O molecules. Since the hypothesis that Fe^{3+} states are formed through oxidation of Fe^{2+} by OH radicals produced by radiolysis of H_2O in hydrated compounds (reaction (1)) is accepted widely, it is reasonably conjectured that one of $Fe^{3+}(1)$ and $Fe^{3+}(2)$ states corresponds to the effect of the nearest H_2O whereas the other is connected with the second nearest H_2O.

The nearest neighbouring H_2O exerts a greater influence on the electric field gradient (EFG) than the further H_2O. Therefore, the greater Q.S. of $Fe^{3+}(2)$ suggests the formation of $Fe^{3+}(2)$ due to radiolysis of the nearest H_2O and the $Fe^{3+}(1)$ states are the effect of the further H_2O. Some of the low-energy Auger electrons which have escaped from the nearest H_2O layer break a second nearest or further H_2O into H and OH radicals. However, contrary to the case of Fe^{2+}, an electron can hardly transfer to this OH radical from the Co^{2+} ion situated close to the OH through the reaction $Co^{2+}+OH \rightarrow Co^{3+}+OH^-$. Therefore, this OH radical oxidize the Fe^{2+} ion, which has emitted the Auger electrons, to form the $Fe^{3+}(1)$ state, or recombines with H after a while.

The energy of the Auger electrons determining the aftereffects is very low (less than a few hundred electron volts), and their range in the lattice is expected very short. Moreover, some of the electrons collide elastically with the H_2O molecules or Cl^- ions in the nearest H_2O layer (without breaking these molecules) and hence loose more energy. Therefore, it is expected

that the stopping power of the electrons is greater on the average in the second nearest or further layer than that in the nearest H_2O layer. Under the coincidence conditions, the number of the emitted Auger electrons is reduced to approximately a half,[10] and therefore the nearest H_2O in the dihydrate sustains hardly radiolysis. This might be the main reason why the $Fe^{3+}(2)$ component is not found in the coincidence spectrum of the dihydrate although the contribution of $Fe^{3+}(1)$ is rather great. In the hexahydrate, owing to the great density of the nearest H_2O, the probability of radiolysis in the nearest H_2O layer is fairly great even under the coincidence conditions. Consequently, both of the Fe^{3+} components appear in the conventional and coincidence spectra.

The appearence of the $Fe^{2+}(2)$ states can actually also be attributed to the effect of the second nearest H_2O. When a OH radical originated outside of the nearest H_2O layer oxidizes Fe^{2+}, it brings about the $Fe^{3+}(1)$ states as mentioned before. On the other hand, when the Fe^{2+} ion does not suffer oxidation by the OH radical in the second nearest H_2O layer, the $Fe^{2+}(2)$ state may appear. In the case that OH survives without recombination with H, the local symmetry around the Fe ion becomes lower and this results in an increase Q.S. value. In the other case that the OH recombines with H, the position of the produced H_2O may differ from its regular crystal site hence may increase the Q.S., as observed for $Fe^{2+}(2)$. Since the second nearest H_2O is less important in the hexahydrate than in the dihydrate, the relative intensity of $Fe^{2+}(2)$ is limited in the conventional spectrum of the hexahydrate. This state is not found in the coincidence spectrum due to the reduced number of the Auger electrons.

The $Fe^{2+}(3)$ state may appear by the effect of the further than second nearest H_2O. The absence of $Fe^{2+}(3)$ in the spectra of the hexahydrate supports this assumption. The unusually small Q.S. can arise from a fortuitous compensation between the lattice and orbital contributions to the EFG. Alternatively, thermal vibration of the localized lattice after the decay of ^{57}Co can conceivably reduce the EFG around Fe^{2+}.

In conclusion, the difference of the emission spectra observed in conventional and in γ-X ray coincidence Mössbauer spectroscopy confirms unambiguously the effectiveness of the Auger and conversion electron self-irradiation in determining the mechanism of stabilization of the anomalous configurations of the decayed atoms. A comparative analysis of the coincidence and regular data in the hydrates $CoCl_2 \cdot 6H_2O$ and $CoCl_2 \cdot 2H_2O$ suggests that the radical reactions involve mostly the nearest neighbour coordination shell in the hexahydrate. In the presence of a lower density of radiosensitive H_2O ligands, as found in the dihydrate, the second nearest coordination shell is also involved in the mechanism of stabilization of the anomalous configurations.

The authors wish to express their thanks to Richard Poinsot for his helpful cooperation.

References

1) R. Ingals, C. J. Coston, G. de Pasquali, H. G. Drickamer, and J. J. Pinajian, *J. Chem. Phys.*, **45**, 1057 (1966).
2) J. M. Friedt, G. K. Shenoy, G. Absteiter, and R. Poinsot, *J. Chem. Phys.*, **59**, 3831 (1973).
3) H. H. Wei, *J. Phys. (Paris), Colloq.*, **40**, C2-426 (1979).
4) J. Ladrière, J. C. Krack, and D. Apers, *J. Phys. (Paris), Colloq.*, **40**, C2-434 (1979).
5) Y. Sakai, K. Endo, and H. Sano, *Bull. Chem. Soc. Jpn.*, **54**, 3587 (1981).
6) D. L. Nagy, R. Doerfler, G. Ritter, J. Waigel, N. Zeman, and B. Molnár, *Phys. Lett.*, **95A**, 400 (1983).
7) J. M. Friedt and J. Danon, *Atom. Energy Rev.*, **18**, 893 (1981).
8) J. Mayer, J. Ladrière, M. Chavee and D. Apers, *J. Phys. (Paris), Colloq.*, **37**, C6-905 (1976).
9) W. Bambynek, B. Crasemann, R. W. Fink, H. U. Freund, H. Mark, C. W. Swift, R. E. Price, and P. V. Rao, *Rev. Mod. Phys.*, **44**, 716 (1972).
10) T. Kobayashi, K. Fukumura, and T. Kitahara, *Nucl. Instrum. Methods*, **166**, 257 (1979).
11) T. Kobayashi, *Radiochim. Acta*, **35**, 43 (1984).
12) F. J. Lynch, R. E. Holland, and M. Hamermesh, *Phys. Rev.*, **120**, 513 (1960).
13) T. Kobayashi and S. Shimizu, *Phys. Lett.*, **54A**, 311 (1975).
14) T. Tominaga and T. Sakai, *Radioisotopes*, **21**, 360 (1972).